

Particle incorporation in metallic melts during dendritic solidification—undercooling experiments under reduced gravity

T. Lierfeld^{a,b,*}, P. Gandham^{a,c}, M. Kolbe^a, T. Schenk^{d,e},
H.M. Singer^f, G. Eggeler^b, D.M. Herlach^a

^a Institute of Space Simulation, German Aerospace Center (DLR), D-51170 Cologne, Germany

^b Institute of Materials, Ruhr-University Bochum, D-44780 Bochum, Germany

^c Department of Metallurgical and Materials Engineering, IITM, Chennai, India

^d Experiments Division (ID19), ESRF, F-38043 Grenoble, France

^e Laboratoire de Physique des Matériaux, EdM de Nancy, F-54042 Nancy, France

^f Laboratory for Solid State Physics, Swiss Federal Institute of Technology ETH, CH-8093 Zurich, Switzerland

Received 21 August 2005; received in revised form 3 February 2006; accepted 23 February 2006

Abstract

The interaction of ceramic particles with a dendritic solid/liquid-interface has been investigated by undercooling experiments with different levels of convection: (i) in a terrestrial electromagnetic levitation facility and (ii) in TEMPUS, a facility for containerless processing, under low gravity conditions during parabolic flights. Entrapment of particles in ground experiments and engulfment of a significant fraction of submicron particles under low gravity conditions are attributed to the lower level of convection in the latter experiments and to morphological features of dendritic solidification. X-ray radiography has been used for in situ observations of directional solidification in $\text{Al}_{90}\text{Cu}_{10}$ with alumina particles. © 2006 Elsevier B.V. All rights reserved.

Keywords: Particle pushing; Dendritic solidification; In situ X-ray radiography; Microgravity; Undercooling

1. Introduction

Since Uhlmann et al. [1] started in 1964, many investigations concerning the interaction of solid particles and a solid/liquid-interface (SLI) during solidification were done [2–5]. Two phenomena have been found for the interaction of particles with a planar s/l-interface:

- (i) particles are pushed by the advancing planar s/l-interface and accumulate in the last solidifying part of the melt (pushing);
- (ii) Particles are engulfed by the advancing planar s/l-interface and are homogeneously incorporated into the solidifying material (engulfing).

For a given particle radius, a transition from (i) to (ii) occurs relatively sharp when the velocity exceeds the critical velocity v_c —this is called the pushing-engulfment-transition (PET). It is known that in general v_c is in the range of $\mu\text{m/s}$ to mm/s and is increased for decreased particle radius [5,6].

On the contrary, the majority of the industrial metallic materials are dendritically solidified, and the knowledge about the interaction of a dendritic s/l-interface with particles is still scarce [6]. Experimental in situ-investigations of the particle pushing phenomenon with dendrites have only been performed in transparent organic model systems [7], but it is not clear, if the results are transferable to technically relevant metal-based systems.

Numerous models have been proposed to describe the particle pushing behaviour: (i) thermodynamic models, (ii) thermal properties criterion models, (iii) kinetic models, and (iv) dynamic models. The first two groups do not predict a critical velocity and therefore they are not considered in the following.

Kinetic models are steady-state models that estimate the critical velocity by a force balance approach. Most of these models

* Corresponding author. Tel.: +49 2203 601 3374; fax: +49 2203 601 2255.
E-mail address: thomas.lierfeld@dlr.de (T. Lierfeld).

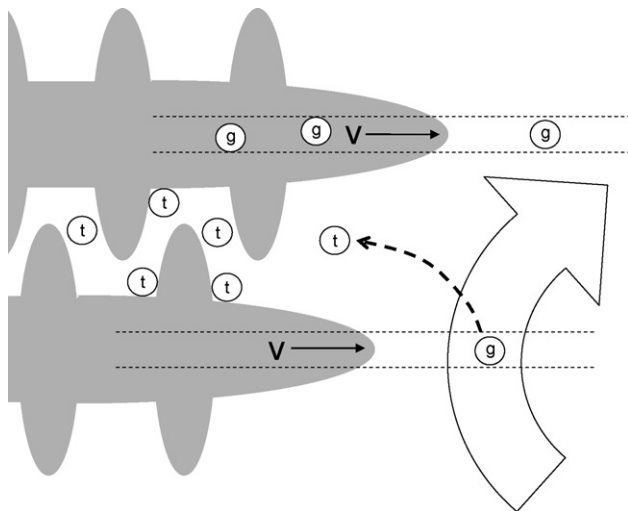


Fig. 1. The morphology of a dendritic s/l-interface permits particle engulfment (g), if a particle is located in a close lateral position to the dendrite tip. Convection moves additional particles into the space between the dendrites, where they might be entrapped (t).

assume no convection as boundary condition. Furthermore, it was reported on increased critical velocities or even absence of particle-interface interaction ($v_c \rightarrow \infty$) in the case of significant melt convection during solidification with a planar SLI [8]. This is explained by additional lift forces caused by the velocity gradient near the SLI. In the case of dendritic solidification the effect of convection might be even more significant. The scenario is sketched in Fig. 1: convection blows away the particles from the moving dendrite tips into the space between the dendrites. Later, they will be found entrapped in the interdendritic region. Thus, the experimental task is to reduce the influence of convection as much as possible.

Dynamic models consider the acceleration of the particle when the SLI approaches. To evaluate these models for real metallic systems, the movement of the particle in the vicinity of the interface needs to be visualized. Sen et al. [9] observed the interaction of a planar SLI in Al with ZrO_2 particles by use of an X-ray transmission microscope. Similar experiments with dendritic solidification front have not yet been performed.

2. Experimental

Our strategy was to investigate the interaction of particles with a dendritic solidification front with two kinds of experiments. First, melt droplets of $\text{Ni}_{98}\text{Ta}_2$ with Ta_2O_5 particles have been undercooled and dendritically solidified. Significant undercooling of the melts has been achieved by (i) electromagnetic levitation (EML, [10]) processing under terrestrial conditions and (ii) in the TEMPUS facility [11] during parabolic flight in low gravity. Electromagnetic levitation on Earth induces strong eddy currents in the melt, which counteract the gravitational forces. This leads to considerable convection in the melt. In TEMPUS during parabolic flight in low gravity, the convection is on a lower level, as has been demonstrated with liquid phase growth experiments of Co–Cu melts [12]. Microstructure analysis after solidification allows the identification of engulfed

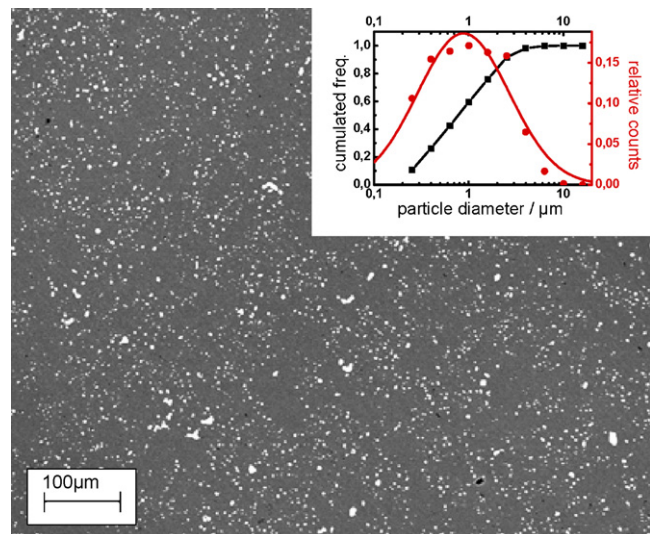


Fig. 2. SEM image of the initial sample material $\text{Ni}_{98}\text{Ta}_2 + \text{Ta}_2\text{O}_5$ particles produced by powder metallurgy.

particles. The velocity of the solidification front can be deduced from the undercooling temperature and dendrite growth velocity measurements.

Second, directional solidification experiments have been conducted with $\text{Al}_{90}\text{Cu}_{10}$ and Al_2O_3 ceramic particles. Synchrotron X-rays were used at Beamline ID19 at the European Synchrotron Radiation Facility (ESRF) Grenoble for in situ visualization of the solidification in a Bridgman furnace with absorption contrast radiography.

The initial samples for levitation processing were prepared by methods of powder metallurgy: powders of nickel, tantalum and tantalum oxide have been mixed in a high purity argon atmosphere, compacted in a hydraulic press with a pressure of 600 MPa to pellets of 1 g, and finally sintered at 1400 $^\circ\text{C}$ for 4–8 h in a high vacuum furnace. The samples have a homogeneous distribution of ceramic particles (Ta_2O_5) in a metallic matrix of $\text{Ni}_{98}\text{Ta}_2$ (Fig. 2).

$\text{Al}_{90}\text{Cu}_{10}$ with Al_2O_3 particles (diameter $d < 44 \mu\text{m}$) has been produced from a sheet of pure aluminium and copper and Al_2O_3 powders. Directional solidification was performed with a thermal gradient of $G = 10 \text{ K/cm}$ and pulling speeds of $v = 2\text{--}10 \mu\text{m/s}$.

3. Results

Post-mortem microstructure analysis of the samples solidified under reduced gravity during parabolic flight shows features on different length scales. On a macroscopic level, particles form open and dense clusters (Fig. 3). Several of the open clusters extend over more than 500 μm in diameter. These structures can be clearly attributed to clustering in the liquid melt before solidification of the sample: we observed the movement of open clusters on the surface of liquid samples during parabolic flight. After the clusters had formed, their shape was stable during the whole period of observation ($\sim 10 \text{ s}$). In ground experiments, the liquid phase period during sample processing has been varied,

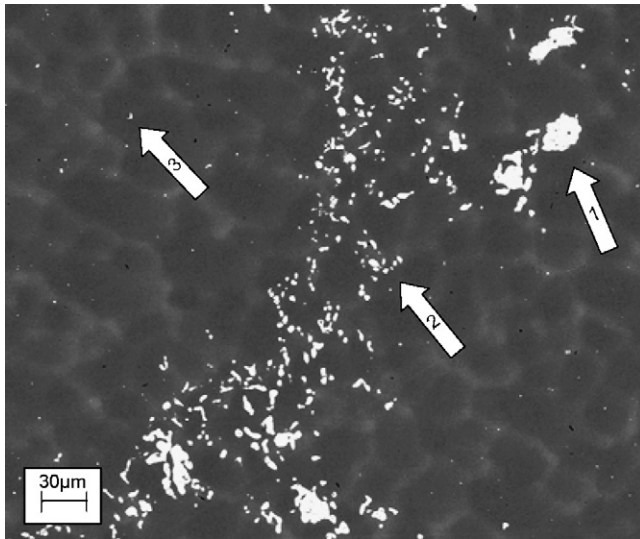


Fig. 3. During parabolic flight processed samples show typically dense (1) and open (2) clusters, as well as single submicron particles (3) in the cluster-free regions. Cluster formation can be clearly attributed to the liquid phase of sample processing and should not be mixed up with pushing of particles.

increased clustering occurs with longer duration of the liquid phase.

On a microscopic scale, single submicron particles can be found in the cluster-free regions (Fig. 3). These particles are located either at the grain boundaries between the dendrites or incorporated into the trunks of dendrites (Fig. 4). This means, particles can be either pushed and/or entrapped between the dendrites or engulfed by the dendrites. For comparison, a typical microstructure obtained by processing under terrestrial conditions is given in Fig. 5. It shows only particles between the dendrites, i.e. particles were pushed and/or entrapped from the growing dendrites. We attribute this difference to the higher

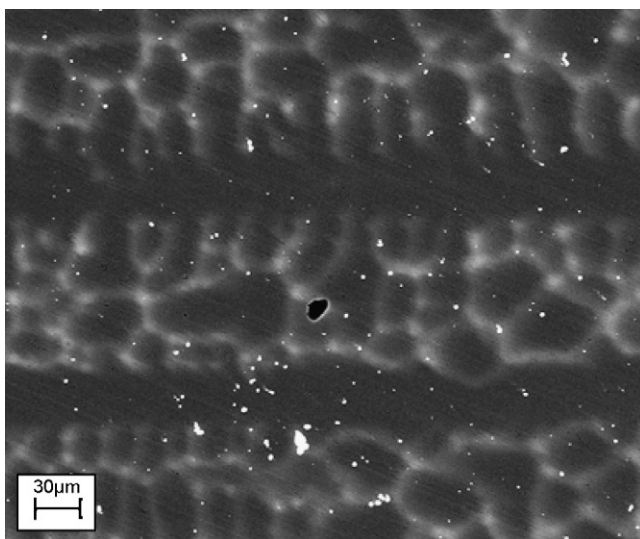


Fig. 4. Typical microstructure of a sample solidified under reduced gravity during parabolic flight. A high fraction of particles is located in the dendrite trunks, as well as in the Ta enriched interdendritic regions (bright). The total particle distribution appears homogeneous; particles are not accumulated in the interdendritic regions.

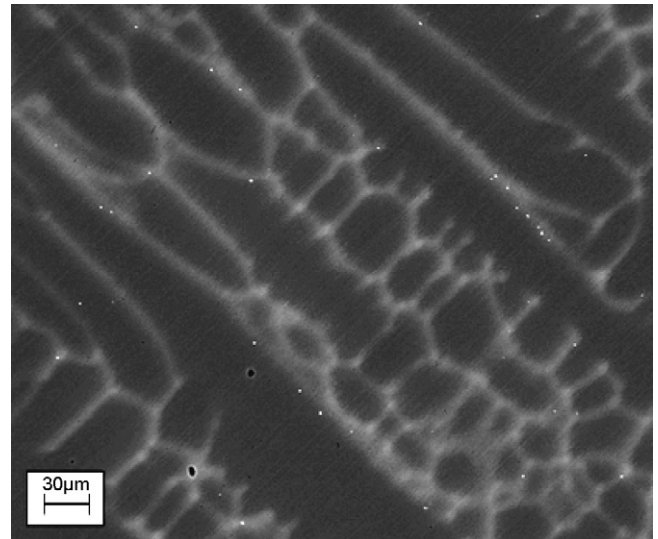


Fig. 5. Typical microstructure of a sample processed in EML under terrestrial conditions. In most cases, particles are entrapped in the interdendritic regions, engulfed particles are very rare.

convection level during solidification in terrestrial processing [12].

A quantitative analysis of the pushed/engulfed particles of samples with different undercoolings from TEMPUS is given in Fig. 6a and b. The normalized size distributions of all particles in the cluster-free regions are compared to the distributions of engulfed particles. The total fraction of engulfed particles is nearly 30% and it is independent from the achieved undercooling and solidification velocity, respectively, in the experimentally accessible range. It shows a weak dependence on the particle diameter: it is constant or even increased for decreasing particle diameter (Fig. 6a and b). It is remarkable that under low gravity conditions, no obvious differences can be found in the size distributions of engulfed particles upon solidification with undercooling of 5 or 84 K.

The results might be interpreted by the following considerations: (i) the scenario, which is shown in Fig. 1, is applicable to the interaction of a dendritic solidification front with particles: if convection is strong, engulfment of particles is not favoured, because the particles are blown away from the growing dendrite tips into the space between the dendrites. Here, continued convection prevents them further from being engulfed by secondary or tertiary dendrite arms. The particles are found entrapped in the last part of the solidifying melt. This behaviour holds for terrestrial EML processing. (ii) Low gravity experiments in TEMPUS allow a reduced convection level. Under these conditions, engulfment of particles is possible by the fast moving dendrite tips or by secondary and tertiary dendrite arms. An estimation of the critical velocities for engulfment following Pötschke and Rogge [4] yields 10–0.2 $\mu\text{m/s}$ for particle diameters 0.1–10 μm . These values are below the velocities of solidification for 5 and 84 K undercooling (0.01 and 7 m/s). A difference in the size distributions could arise at particle diameters below 0.1 μm . (iii) It is reasonable to assume that residual convection is present between the dendrites even in low gravity.

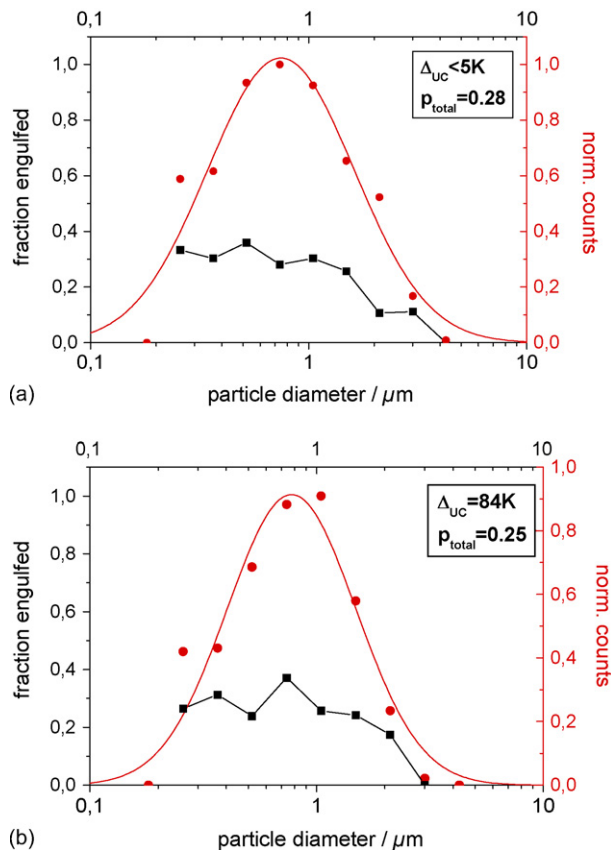


Fig. 6. Normalized particle size distribution and fraction of engulfed particles in cluster-free regions of two samples with different level of undercooling (5 and 84 K) processed during parabolic flight. Note, that the fraction of engulfed particles does not change with the level of undercooling.

Therefore, a fraction of particles is entrapped between the dendrites.

The aim of our in situ X-ray imaging experiments is to observe the particle interaction with a dendritic SLI. The challenge is to find a system where contrast arises between solidified material, melt, and particles, and at the same time, the buoyancy between particle and melt is neglectable.

Many details of solidification were observed during the experiments, especially: (i) splitting of dendrite tips and (ii) development of cauliflower morphology. Unfortunately, the alumina particles could not be visualized because of low contrast and a speckled background, which is due to the carbon containment. Tip splitting possibly indicates the presence of particles, since it is one of the proposed mechanisms for particle incorporation in the dendritic case [7].

Post-mortem scanning electron microscopy (SEM) analysis did not support the involvement of particles in the change of dendrite growth morphology. Particles are incorporated in the interdendritic eutectic region, which means that they have been pushed and/or entrapped. The critical velocity calculated for the planar case with the Pötschke–Rogge model [4] is below $0.1 \mu\text{m/s}$, thus, in the planar case, engulfment would occur for a solidification velocity of $v = 5 \mu\text{m/s}$ used for this sample. In the

dendritic case, entrapment is favoured probably due to the mechanism proposed in Fig. 1. The observed dendrite morphologies might be explained by the low anisotropy of solid/liquid interfacial energy in $\text{Al}_{90}\text{Cu}_{10}$ [13,14].

4. Summary

The interaction of a dendritic solid/liquid-interface with inert particles has been investigated in the TEMPUS facility during parabolic flight and in a terrestrial EML facility in $\text{Ni}_{98}\text{Ta}_2$ with Ta_2O_5 particles. Undercooling of the melt has been achieved in both cases, the solidified microstructures show significant differences: the particles are found in clusters and as isolated particles; whereas they are nearly all entrapped after terrestrial experiments, low gravity conditions lead to engulfment of about 30% of the isolated particles in the cluster-free regions. The results of the low gravity experiments are independent from undercooling in the range from 5 to 84 K. It is assumed that the lower level of convection during parabolic flights allows engulfment of particles by a dendritic solidification front. A mechanism is proposed, which takes into account convection and dendrite morphology. It is planned to conduct undercooling experiments in MSL-EML on board of the International Space Station ISS, where the convection level could be further decreased.

Acknowledgements

The work was performed in the frame of ESA MAP “METCOMP”. Financial support of ESA (14243/00/NL/SH) and DLR (50 WM 0121) is gratefully acknowledged. We acknowledge the European Synchrotron Radiation Facility for provision of synchrotron radiation facilities and for assistance in using beamline ID 19. One of the authors (PG) acknowledges support through research fellowship from the Alexander von Humboldt Foundation.

References

- [1] D.R. Uhlmann, B. Chalmers, K.A. Jackson, *J. Appl. Phys.* 35 (1964) 2986.
- [2] S.N. Omenyi, A.W. Neumann, *J. Appl. Phys.* 47 (1976) 3956.
- [3] D.M. Stefanescu, B.K. Dhindaw, S.A. Kacar, A. Moitra, *Metall. Trans. A* 19 (1988) 2847.
- [4] J. Pötschke, V. Rogge, *J. Cryst. Growth* 94 (1989) 726.
- [5] R. Asthana, R.N. Tewari, *J. Mater. Sci.* 28 (1993) 5414.
- [6] D.M. Stefanescu, *Science and Engineering of Casting Solidification*, Kluwer Academic/Plenum Publishers, New York, 2002.
- [7] J.A. Sekhar, R. Trivedi, *Mater. Sci. Eng. A* 147 (1991) 9.
- [8] D.M. Stefanescu, F.R. Juretzko, B.K. Dhindaw, A. Catalina, S. Sen, P.A. Curreri, *Metall. Mater. Trans. A* 29 (1998) 1697.
- [9] S. Sen, W.F. Kaukler, P. Curreri, D.M. Stefanescu, *Metall. Mater. Trans. A* 28 (1997) 2129.
- [10] D.M. Herlach, R. Willnecker, F. Gillesen, in: *Proceedings of the Fifth European Symposium on ‘Material Sciences under Microgravity’*, Schloss Elmau, 1984, ESA SP-222, pp. 399–403.
- [11] G. Lohöfer, J. Piller, *Proceedings of the 40th AIAA Aerospace Sciences Meeting & Exhibit*, 14–17 January, 2002, Reno, NV, AIAA 2002-0764.
- [12] M. Kolbe, J.R. Gao, *Mater. Sci. Eng. A* 413–414 (2005) 509.
- [13] L. Shan, R.E. Napolitano, R. Trivedi, *Acta Mater.* 49 (2001) 4271.
- [14] S. Henry, P. Jarry, M. Rappaz, *Metall. Mater. Trans. A* 29 (1998) 2807.